Eur. Phys. J. C 6, 437–450 (1999)
DOI 10.1007/s100529801032

THE EUROPEAN PHYSICAL JOURNAL C

Pion correlations and resonance effects in $\bar{p}p$ annihilation at rest to $2\pi^+2\pi^-\pi^0$

CPLEAR Collaboration

A. Apostolakis[1], E. Aslanides[11], G. Backenstoss[2], P. Bargassa[13], O. Behnke[17], A. Benelli[2], V. Bertin[11], F. Blanc[7,13], P. Bloch[4], P. Carlson[15], M. Carroll[9], E. Cawley[9], M.B. Chertok[3], M. Danielsson[15], M. Dejardin[14], J. Derre[14], A. Ealet[11], C. Eleftheriadis[16], L. Faravel[7], W. Fetscher[17], M. Fidecaro[4], A. Filipčič[10], D. Francis[3], J. Fry[9], E. Gabathuler[9], R. Gamet[9], H.-J. Gerber[17], A. Go[15], A. Haselden[9], P.J. Hayman[9], F. Henry-Couannier[11], R.W. Hollander[6], K. Jon-And[15], P.-R. Kettle[13], P. Kokkas[4], R. Kreuger[6], R. Le Gac[11], F. Leimgruber[2], I. Mandić[10], N. Manthos[8], G. Marel[14], M. Mikuž[10], J. Miller[3], F. Montanet[11], A. Muller[14], T. Nakada[13], B. Pagels[17], I. Papadopoulos[16], P. Pavlopoulos[2], G. Polivka[2], R. Rickenbach[2], B.L. Roberts[3], T. Ruf[4], L. Sakeliou[1], M. Schäfer[17], L.A. Schaller[7], T. Schietinger[2], A. Schopper[4], L. Tauscher[2], C. Thibault[12], F. Touchard[11], C. Touramanis[4], C.W.E. Van Eijk[6], S. Vlachos[2], P. Weber[17], O. Wigger[13], M. Wolter[17], D. Zavrtanik[10], D. Zimmerman[3],

and

M.P. Locher[18], V.E. Markushin[18]

[1] University of Athens, Greece
[2] University of Basle, Switzerland
[3] Boston University, USA
[4] CERN, Geneva, Switzerland
[5] LIP and University of Coimbra, Portugal
[6] Delft University of Technology, Netherlands
[7] University of Fribourg, Switzerland
[8] University of Ioannina, Greece
[9] University of Liverpool, UK
[10] J. Stefan Inst. and Phys. Dep., University of Ljubljana, Slovenia
[11] CPPM, IN2P3-CNRS et Université d'Aix-Marseille II, France
[12] CSNSM, IN2P3-CNRS, Orsay, France
[13] Paul Scherrer Institut (PSI), Villigen, Switzerland
[14] CEA, DSM/DAPNIA, CE-Saclay, France
[15] Royal Institute of Technology, Stockholm, Sweden
[16] University of Thessaloniki, Greece
[17] ETH-IPP Zürich, Switzerland
[18] Paul Scherrer Institut (PSI), Theory Group F1, Villigen, Switzerland

Received: 4 August 1998 / Published online: 6 November 1998

Abstract. We study $\pi\pi$ correlations in the exclusive reaction $\bar{p}p \to 2\pi^+2\pi^-\pi^0$ at rest with complete reconstruction of the kinematics for each event. Inclusive and differential distributions properly normalized show an enhancement for small invariant masses M_{++},M_{--} of like-pion pairs. An even stronger enhancement is seen for the double differential distributions for low pion-pair masses. The signal is strongest when the π^0 energy is large and much weaker when this energy is small. Dynamical models with resonances in the final state are confronted with the data. For the kinematic situation where the $\rho 3\pi$ channel is important the simulation predicts a large pion correlation for the double differential density, qualitatively explaining the observed bahaviour. The stochastic HBT mechanism is not supported by these findings for the exclusive annihilation reaction studied.

1 Introduction

Nucleon-antinucleon annihilation into multipion states offers the possibility of studying Bose-Einstein (BE) symmetrization effects under controlled conditions. In [1] we have studied the exclusive reaction $\bar{p}p \to 2\pi^+2\pi^-$ at rest on the basis of minimum bias CPLEAR data. The complete kinematical reconstruction of each event has allowed the direct determination of the square of the reaction amplitude. It was found that inclusive densities for equal charge pairs show very little enhancement at low invariant pion pair mass M where signals are expected. In contrast

to this the double-differential distribution in the two equal charge pairs shows a conspicuous signal at low invariant masses of the two pairs. This signal is washed out by the integration leading to the inclusive single pair distribution. For the quantitative aspects it is important not to rely on unequal charge pion pairs as reference sample since $\pi^+\pi^-$ pairs are strongly depleted at low pair masses by the presence of the ρ meson resonance.

The present paper extends the four pion analysis of [1] to the annihilation reaction $\bar{p}p \to 2\pi^+2\pi^-\pi^0$ at rest. This allows us to study the signal as a function of the total energy in the system of the four charged pions. We have generalized the formalism of [1] to the five pion case and studied both the inclusive and the double differential distributions as a function of the invariant masses of the pion pairs in different kinematical regions.

The inclusive correlation signal is found to be stronger in the 5π case than in the 4π channel, but similar otherwise. In particular inclusive correlations are partly washed out by the integration over the remaining phase space. The twofold differential distributions on the other hand, show a strong enhancement at low invariant mass of like-pion pairs where signals of pion correlations are expected. The detailed analysis of the differential distribution shows a marked dependence of the correlation signal on the invariant mass M_{++--} of the $2\pi^+2\pi^-$ system: it is strong at small values of M_{++--} (large π^0 energies) and decreases with increasing M_{++--}. As we shall discuss, this energy dependence, as well as the strength and the shape of the signal do not favour an interpretation in terms of the conventional Hanbury–Brown-Twiss (HBT) [2–5] picture of BE correlations. This conclusion is based on simulations of resonance production in the final state which qualitatively explain a large part of the observed effects.

The plan of the paper is as follows. In Sect. 2 we describe the analysis of the data and the results for the single variable distributions. The extension of the formalism of differential distributions to the five pion channel is given in Sect. 3 that shows the presence of the correlation signal in the double-differential distributions. Section 4 discusses the results comparing with detailed model calculations including the dominant resonance mechanisms. Partial projections similar to the analysis performed earlier in the $2\pi^+2\pi^-$ case are shown as well and confronted with dynamical models. Section 5 gives a summary and conclusions.

2 Analysis of the $2\pi^+2\pi^-\pi^0$ data

The reaction $\bar{p}p \to 2\pi^+2\pi^-\pi^0$ at rest in the CPLEAR experiment proceeds from S- and P-wave atomic states [6]. The corresponding pion distribution for the final state configuration $\{\mathbf{p}_i\}$, $i = 1, 2, \ldots, 5$, has the form

$$d\sigma(\{\mathbf{p}_i\}) \sim |T(\mathbf{k}, \{\mathbf{p}_i\})|^2_{\mathbf{k}\to 0}\, d\Phi_5(p, p_1, p_2, p_3, p_4, p_5) \quad (1)$$

Here $T(\mathbf{k}, \{\mathbf{p}_i\})$ is the amplitude of the $\bar{p}p$ annihilation from the initial $\bar{p}p$ state with relative momentum $\mathbf{k}$, $d\Phi_5(p, p_1, p_2, p_3, p_4, p_5)$ is the 5-body relativistic phase space, and the limit $\mathbf{k} \to 0$ implies the incoherent addition of the S- and P-wave annihilation occurring in the experiment. The four-vectors of the pions are $p_i = (E_i, \mathbf{p}_i)$, and $p = (2m_p, 0)$ is the total four-momentum for $\bar{p}p$ annihilation at rest, m_p being the proton mass. The notation implies a sum over initial spin states, and all quantum numbers specifying the initial spin and orbital momentum are suppressed.

2.1 Event selection

The CPLEAR detector [7] is cylindrically symmetric and placed inside a solenoidal magnet of 3.6 m length and 2 m diameter, with a field of 0.44 T. Antiprotons of 0.2 GeV/c momentum, provided by LEAR, stop and annihilate at the centre of the detector, in a spherical target of 7 cm radius filled with gaseous hydrogen at 16 bar. Tracking is provided by two layers of proportional chambers, six layers of drift chambers, and two layers of streamer tubes. Outside the tracking devices there are 32 sectors of Scintillator (S1) – Cherenkov (C) – Scintillator (S2) sandwiches providing particle identification. The outermost detector is an 18-layer lead/gas-sampling electromagnetic calorimeter.

The data analysed here represent a small fraction of the CPLEAR data and were collected with the so-called *minimum-bias trigger* in 1993 and 1994[1]. This trigger requires a hit in the scintillator S1 in coincidence with the incoming antiproton and accepts events in the entire phase space, limited only by the energy thresholds and geometrical acceptances. From the total of about $5.5{\cdot}10^7$ minimum-bias events, well balanced between opposite magnetic-field polarity settings, $0.94{\cdot}10^7$ four-prong events were selected according to the following criteria:

1. four tracks balanced in charge;
2. good quality of track reconstruction (minimal number of tracking hits, good χ^2 for the track fit) and the vertex coordinates of all track pairs inside the target sphere.

All tracks were assumed to be pions. The photons from the $\pi^0 \to 2\gamma$ decay were not considered in the event selection. The π^0 kinematics was thus reconstructed from the charged pions by the missing momentum technique. To select exclusively the events of the $2\pi^+2\pi^-\pi^0$ channel, kinematical and topological cuts were applied:

1. the 4π invariant mass $m_{4\pi}$ is required to be $m_{4\pi} < 1.70$ GeV to reject events from the $2\pi^+2\pi^-$ channel;
2. the momentum of each track (pion) must be in the range $0.06 \le p_\pi \le 0.92$ GeV/c;
3. the 5π invariant mass

$$m_{5\pi} = \sum_{i=1}^{4} \sqrt{m^2_{\pi^\pm} + \mathbf{p}_i^2} + \sqrt{m^2_{\pi^0} + (\sum_{i=1}^{4} \mathbf{p}_i)^2} \quad (2)$$

must be within the mass interval 1.87 GeV $< m_{5\pi} <$ 1.98 GeV.

[1] The data published earlier in [8] were collected in 1991 and 1992 with the same trigger

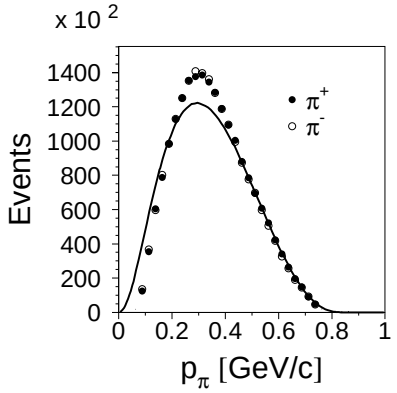

Fig. 1. The measured single-pion momentum distribution $dN_\pi/d|\mathbf{p}_\pi|$ for the $2\pi^+2\pi^-\pi^0$ channel. The values are shown for π^+ (•) and π^- (○). The line is the phase-space distribution

4. an opening angle ≥ 60 mrad is required between any two charged tracks to avoid pion pairs with insufficient two-track resolution and lepton pairs from γ conversion and π^0 Dalitz decays.

Since only charged pions have been analysed, the selection of $2\pi^+2\pi^-\pi^0$ events is less well defined than in the previous search for $2\pi^+2\pi^-$ events. Thus many annihilation channels were considered and studied as possible source of background. The process $\bar{p}p \to 2\pi^+2\pi^-2\pi^0$ with a branching ratio similar to $2\pi^+2\pi^-\pi^0$ was found by MC simulation to be the strongest background channel, i.e. the tails of $m_{5\pi}(2\pi^+2\pi^-2\pi^0)$ did extend into the signal region because of the finite momentum resolution. Monte Carlo simulations showed that with the above cuts our data sample contains about 5% background from $2\pi^+2\pi^-2\pi^0$, 0.5% from $2\pi^+2\pi^-$, and less than 1% from other annihilation channels. Especially the contamination with charged kaons is found to be small. No evidence for neutral kaons can be found in the data, where the decays of $K_S \to \pi^+\pi^-$ would leave a prominent (narrow) signal. A total of $8.3{\cdot}10^5$ $2\pi^+2\pi^-\pi^0$ events remained. The single-track momentum resolution is about 5%, and a resolution of $\sigma(M^2) \leq 0.005$ GeV^2 is achieved in the region of interest (low M^2). A typical bin width is 0.02 GeV^2 for integrated spectra and 0.05 GeV^2 for differential spectra.

The measured pion momentum distributions for π^+ and π^- are plotted in Fig. 1. The perfect agreement between these two spectra shows that there are no systematic differences. The shape of the momentum distribution is quite close to phase space which is also shown in Fig. 1.

Figures 2a–d show the measured distributions in the invariant masses of the $\pi^+\pi^-$, $\pi^\pm\pi^0$ and $\pi^+\pi^-\pi^0$ systems (the plot (a) contains all combinatorial contributions, i.e. 4 entries per event). A strong signal from the $\rho\omega$ channel is clearly seen in Figs. 2a,b; we shall discuss this feature in Sect. 4.

2.2 Correlation functions for inclusive distributions

The single-particle inclusive density $\rho_1(p_1)$ and the two-particle inclusive density $\rho_2(p_1, p_2)$ are related to the differential cross-sections by

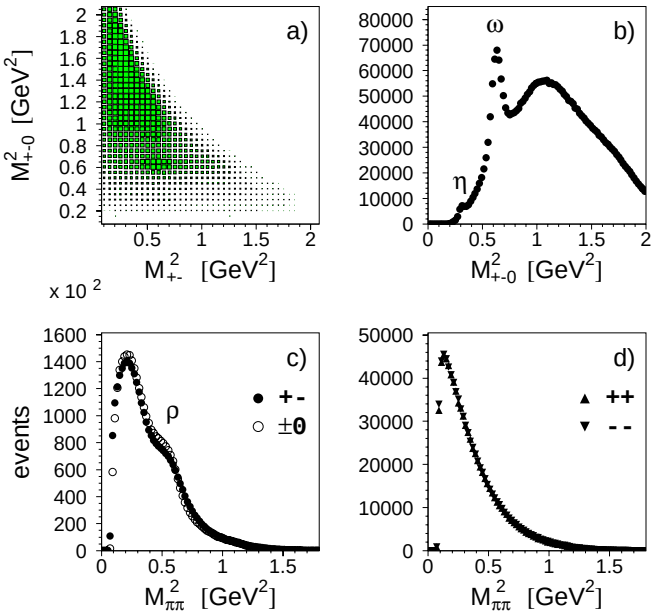

Fig. 2. The measured mass distributions for the reaction $\bar{p}p \to 2\pi^+2\pi^-\pi^0$: **a** the double-differential spectrum $dN/dM^2_{+-}dM^2_{+-0}$ as a function of the invariant masses of the $\pi^+\pi^-$ and $\pi^+\pi^-\pi^0$ systems, **b** the spectrum of the $\pi^+\pi^-\pi^0$ invariant mass, **c** the spectra of the $\pi^+\pi^-$ (•) and $\pi^\pm\pi^0$ (○) invariant masses, **d** the spectrum of the $\pi^+\pi^+$ and $\pi^-\pi^-$ invariant masses

$$\rho_1(p_1) = \sigma^{-1}\frac{d\sigma}{d^3\mathbf{p}_1/2E_1} \tag{3}$$

$$\rho_2(p_1,p_2) = \sigma^{-1}\frac{d\sigma}{d^3\mathbf{p}_1/(2E_1)\; d^3\mathbf{p}_2/(2E_2)} \quad . \tag{4}$$

One of the definitions of pion pair correlations is based on the formula

$$c(p_1,p_2) = \rho_2(p_1,p_2) - \rho_1(p_1)\rho_1(p_2) \quad . \tag{5}$$

Alternatively the two-particle correlations can be described in terms of the ratio

$$C(p_1,p_2) = \frac{\rho_2(p_1,p_2)}{\rho_0(p_1,p_2)} \quad , \tag{6}$$

where $\rho_0(p_1,p_2)$ is the two-particle distribution *in the absence of correlations*, with various prescriptions being used in the literature. One choice, consistent with (5), is the product of the single-particle densities $\rho_0(p_1,p_2) = \rho_1(p_1)\,\rho_1(p_2)$. Another choice of reference sample, mentioned in the introduction, is to take the two-particle inclusive distribution for *unlike* pions: $\rho_0(p_1,p_2) = \rho_2^{+-}(p_1,p_2)$ [8–11]. In this case some experimental uncertainties cancel out in the ratio $R_2(p_1,p_2) = \rho_2^{++|--}(p_1,p_2)/\rho_2^{+-}(p_1,p_2)$. However, the correlation function thus calculated is known to be distorted by the dynamics for particles of unlike charge [10, 1].

Averaging over angles and momenta gives correlation functions depending on one parameter, i.e. the two-pion

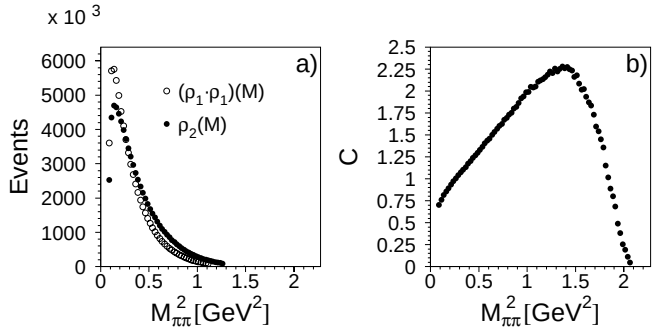

Fig. 3. The calculated effective-mass distributions **a** $\rho_2(M)$ and $(\rho_1 \cdot \rho_1)(M)$ for $\bar{p}p \to 5\pi$ at $\sqrt{s} = 2m_p$, assuming a pure phase-space distribution, **b** the corresponding correlation function $C(M)$

invariant mass M:

$$C(M) = \frac{\rho_2(M)}{(\rho_1 \cdot \rho_1)(M)} \tag{7}$$

$$\rho_2(M) = \int \delta\left(M - \sqrt{(p_1+p_2)^2}\right) \rho_2(p_1,p_2) \times \frac{d^3\mathbf{p}_1 d^3\mathbf{p}_2}{(2E_1)(2E_2)} \tag{8}$$

$$(\rho_1 \cdot \rho_1)(M) = \int \delta\left(M - \sqrt{(p_1+p_2)^2}\right) \rho_1(p_1)\rho_1(p_2) \times \frac{d^3\mathbf{p}_1 d^3\mathbf{p}_2}{(2E_1)(2E_2)} \tag{9}$$

The invariant mass M is uniquely related to the square of the momentum difference:

$$(p_1 - p_2)^2 = 4\mu^2 - M^2 = -Q^2, \tag{10}$$

where μ is the pion mass and $\mathbf{Q}$ is the difference of the three-momenta of the two pions in their centre-of-mass system (CMS), therefore the variables M^2 and Q^2 are equivalent.

Because of the total energy-momentum conservation, the ratio $C(M)$ is not a constant even if the distributions $d\sigma/(d^3\mathbf{p}_1/2E_1)$ and $d\sigma/(d^3\mathbf{p}_1/2E_1)(d^3\mathbf{p}_2/2E_2)$ are determined by phase space alone. This purely kinematical effect is especially strong for the $\bar{p}p$ annihilation at rest[2], as shown in Fig. 3 for the annihilation into five pions. Therefore these *kinematical* correlations must be removed from the correlation function $C(M)$ in order to reveal the dynamics of the pion production.

2.3 Single-variable two-pion correlations

In this subsection we present the single-variable two-pion correlations $R_2(M)$ and $C(M)$ which have been frequently used in previous analyses. In order to isolate the correlation effects we compare the experimental density with a five-pion phase space distribution corrected for experimental cuts and efficiencies in the same way as the data.

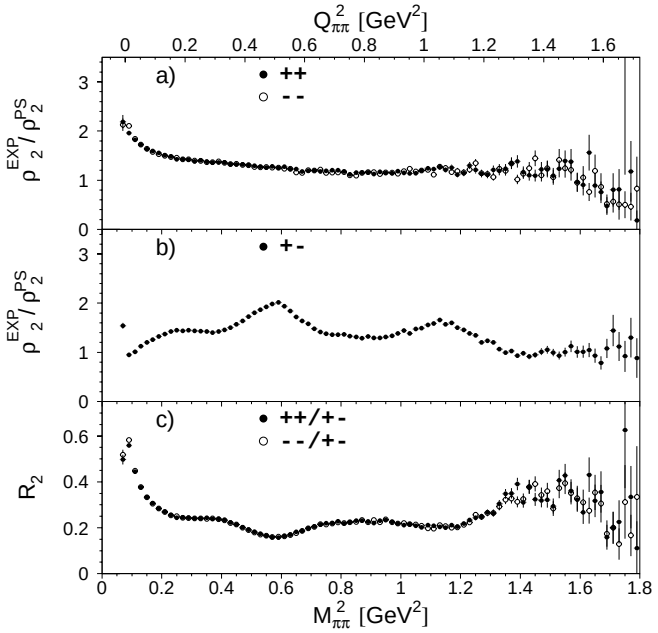

Fig. 4a–c. Inclusive experimental two-pion correlations *vs.* the effective mass squared M^2 of the pion pair in the $2\pi^+2\pi^-\pi^0$ channel. Two-particle distributions $\rho_2(M)$, (8), divided by phase space $\rho_2^{PS}(M)$: **a** pairs of identical pions, $\pi^+\pi^+$ (•) and $\pi^-\pi^-$ (○), **b** pairs of unlike pions, **c** the ratio R_2 of the experimental two-particle distributions for like and unlike pions: $\rho_2^{++}(M)/\rho_2^{+-}(M)$ (•) and $\rho_2^{--}(M)/\rho_2^{+-}(M)$ (○)

The data sample of $8.3 \cdot 10^5$ events was used to calculate the two-particle distributions $\rho_2(M)$ defined by (8) for pairs of identical pions, $\rho_2^{++}(M)$ and $\rho_2^{--}(M)$, and pairs of unlike pions[3], $\rho_2^{+-}(M)$. The corresponding two-particle density from the phase-space simulation is called $\rho_2^{PS}(M)$. In Figs. 4a and 4b we consider the ratios of distributions for like- and unlike-pion pairs normalized to phase space, $\rho_2^{++|--|+-}(M)/\rho_2^{PS}(M)$, for which the kinematical correlations discussed in Sect. 2.2 cancel. The ratios $\rho_2^{++}(M)/\rho_2^{PS}(M)$ and $\rho_2^{--}(M)/\rho_2^{PS}(M)$ shown in Fig. 4a peak at small Q^2. Note that this peak is stronger than that in the $\bar{p}p \to 2\pi^+2\pi^-$ case [1].

Figure 4c shows the ratio of experimental two-particle distributions

$$R_2(M) = \frac{\rho_2^{++|--}(M)}{\rho_2^{+-}(M)} \quad . \tag{11}$$

The results for $R_2(M)$ are consistent with those previously reported [8]. Comparing Figs. 4a and 4b with Fig. 4c one sees that the peak in $R_2(M)$ is partly due to the strong depletion of the unequal charge distribution at small Q^2 which is due to the presence of ρ mesons and other resonances, absent in the $\pi^+\pi^+$ and $\pi^-\pi^-$ channels. It is therefore dangerous to deduce model parameters from the

[2] In high energy reactions this effect is not significant, if the two pions carry a small fraction of the total energy

[3] Here and below all distributions for unlike-pion pairs contain multiple entries per event corresponding to all possible $\pi^+\pi^-$ combinations

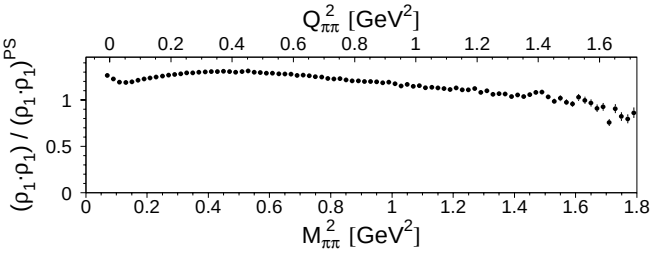

Fig. 5. The ratio of the experimental distribution $(\rho_1 \cdot \rho_1)(M)$ to the phase-space distribution $(\rho_1 \cdot \rho_1)^{PS}(M)$

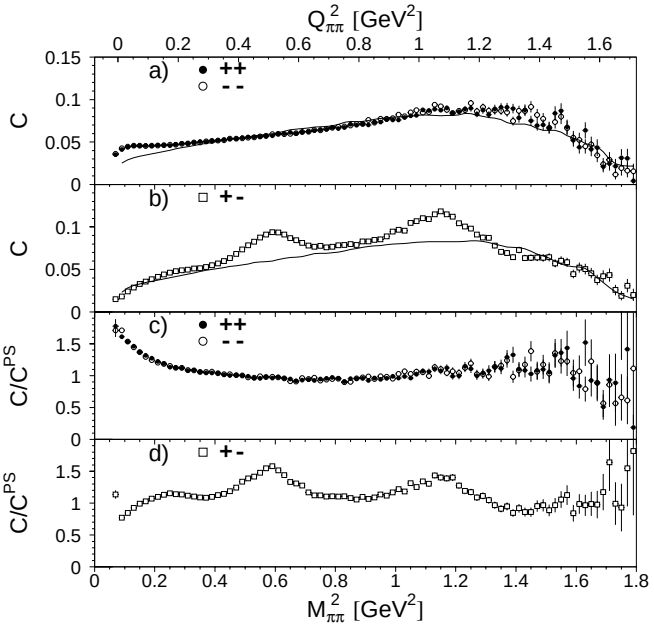

Fig. 6. The experimental correlation function $C(M)$, (7), *vs.* the square of the effective mass M^2 of two pions in the $2\pi^+2\pi^-\pi^0$ channel: **a** $\rho_2^{++}(M)/(\rho_1 \cdot \rho_1)(M)$ (•) and $\rho_2^{--}(M)/(\rho_1 \cdot \rho_1)(M)$ (○), **b** $\rho_2^{+-}(M)/(\rho_1 \cdot \rho_1)(M)$ (□). The lines in **a** and **b** show the corresponding phase-space ratio $\rho_2^{PS}(M)/(\rho_1 \cdot \rho_1)^{PS}(M)$. The experimental correlation functions normalized to the phase-space distribution, $C(M)/C^{PS}(M)$, (12), are shown in **c** for $\pi^+\pi^+$ (•) and $\pi^-\pi^-$ (○), and in **d** for $\pi^+\pi^-$

ratio $R_2(M)$, as has been discussed many times [1,5,12, 15].

To study the correlation function $C(M)$ in (7), the two-particle distribution for uncorrelated pion pairs was calculated using the same event-mixing method as in [1]. The experimental distribution $(\rho_1 \cdot \rho_1)(M)$ normalized to phase space (see below) is plotted in Fig. 5. Separate $(\rho_1 \cdot \rho_1)(M)$ distributions were analysed for $++$, $--$, and $+-$ pion pairs and all found to be consistent. All these distributions are found to be quite flat in the region of interest as it should be. Figures 6a,b show the correlation functions $C(M)$ for like and unlike pion pairs. In order to account for the trivial M-dependence which arises from the energy-momentum conservation for the pure phase-space distribution (see Fig. 3) and from the experimental cuts,

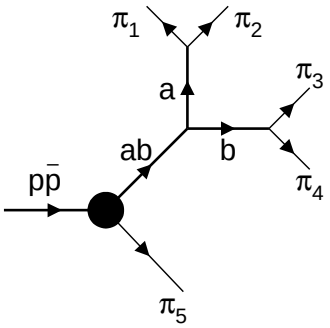

Fig. 7. The two-pion subsystems $a = (\pi_1 + \pi_2)$ and $b = (\pi_3 + \pi_4)$ in the five pion final state ($\pi_5 = \pi^0$)

the following double ratio has been calculated:

$$\frac{C^{++|--|+-}(M)}{C^{PS}(M)} = \frac{\rho_2^{++|--|+-}(M)}{(\rho_1 \cdot \rho_1)(M)} : \frac{\rho_2^{PS}(M)}{(\rho_1 \cdot \rho_1)^{PS}(M)} \,. \qquad (12)$$

The result is shown in Figs. 6c,d. The ratios $C^{++}(M)/C^{PS}(M)$ and $C^{--}(M)/C^{PS}(M)$ display a clear enhancement at low effective mass of like-charge pion pairs. The distributions in Figs. 6c,d resemble very much the distributions in Figs. 4a,b obtained in a very different manner.

3 Differential two-pion correlations

So far we have presented the inclusive correlation functions $C^{++|--}(M)/C^{PS}(M)$ where all kinematical variables except M have been integrated out. To investigate the correlation signal in more detail we turn to differential densities. Our approach generalizes the method used previously for the four-pion system [1].

We introduce the two-pion subsystems a and b with four-momenta $p_a = (p_1 + p_2)$ and $p_b = (p_3 + p_4)$ and invariant masses M_a and M_b, see Fig. 7. The invariant mass of the four-pion system with the total four-momentum $p_{ab} = (p_1 + p_2 + p_3 + p_4)$ is $M_{ab} = \sqrt{p_{ab}^2}$ recoiling against the π^0 with the four-momentum p_5. Using the reduction formula for the 5-body phase space

$$d\Phi_5(p, p_1, p_2, p_3, p_4, p_5) = d\Phi_4(p_{ab}, p_1, p_2, p_3, p_4) d\Phi_2(p, p_{ab}, p_5)(2\pi)^3 dp_{ab}^2 \,, \qquad (13)$$

the differential cross section of (1) can be written in the form

$$d\sigma \sim |T(\mathbf{k}, \{\mathbf{p}_i\})|^2_{\mathbf{k}\to 0} d\Phi_4(p_{ab}, p_1, p_2, p_3, p_4) \times d\Phi_2(p, p_{ab}, p_5) dM_{ab}^2 \,. \qquad (14)$$

Given the invariant masses M_a, M_b, and M_{ab}, the triple differential cross section is defined by integrating over the angles specifying the relative orientation of the momenta of the pions within the subsystems a and b, the relative orientation of the subsystems a and b, and the

direction of the 5-th pion (the corresponding solid angles are $d\Omega_{12}$, $d\Omega_{34}$, $d\Omega_{ab}$, and $d\Omega_5$). Two types of subsytems a and b will be used which are distinguished by the explicit labels of the pion charges: the case of like-pion pairs corresponds to $M_a = M_{++}$ and $M_b = M_{--}$, and the case of unlike-pion pairs to $M_a = M_{+-(a)}$ and $M_b = M_{+-(b)}$. The 5-th pion is always π^0, and the notation $M_{ab} = M_{++--}$ will be used to indicate explicitly that there are only charged pions in the subsytems a and b.

For the reaction $\bar{p}p \to 2\pi^+2\pi^-\pi^0$ we have

$$\frac{d\sigma}{dM_{ab}^2 dM_a^2 dM_b^2} \sim W\left(M_{ab}, M_a, M_b\right) P\left(\sqrt{s}, M_{ab}, \mu\right) \times \int |T(\mathbf{k}, \{\mathbf{p}_i\})|^2_{\mathbf{k}\to 0}\, d\Omega_{ab} d\Omega_{12} d\Omega_{34} d\Omega_5 \quad (15)$$

where $P(M, M_x, M_y)$ is the relative momentum of two particles with masses M_x and M_y and the total invariant mass M

$$P(M, M_x, M_y) = \frac{\sqrt{(M^2 - (M_x + M_y)^2)(M^2 - (M_x - M_y)^2)}}{2M} . \quad (16)$$

The factor $W(M_{ab}, M_a, M_b)$ is given by

$$W(M_{ab}, M_a, M_b) = \frac{P_{ab}}{M_{ab}} \sqrt{\left(1 - \frac{4\mu^2}{M_a^2}\right)\left(1 - \frac{4\mu^2}{M_b^2}\right)} , \quad (17)$$

$$P_{ab} = P(M_{ab}, M_a, M_b) . \quad (18)$$

Removing the phase-space factor $W(M_{ab}, M_a, M_b)$, we define the triple differential density:

$$\varrho(M_{ab}, M_a, M_b) = \frac{1}{W(M_{ab}, M_a, M_b)} \times \frac{d\sigma}{\sigma \cdot dM_{ab}^2 dM_a^2 dM_b^2} \quad (19)$$

$$\sim P(\sqrt{s}, M_{ab}, \mu) \times \int |T(\{\mathbf{p}_i\})|^2 d\Omega_{ab} d\Omega_{12} d\Omega_{34} d\Omega_5 \quad (20)$$

where σ is the total cross section.

An advantage of using the triple differential density $\varrho(M_{ab}, M_a, M_b)$ is that it does not contain *kinematical* dependences on the invariant masses of the two-pion pairs a and b. This means that for a constant T matrix the density $\varrho(M_{ab}, M_a, M_b)$ does not depend on M_a and M_b, contrary to $\rho_2(M_a) = d\sigma/dM_a$ of (8). By integrating over the invariant mass of the four-pion system, M_{ab}, within the interval $[M_{ab}^{min}, M_{ab}^{max}]$ we get the integrated two-dimensional density

$$\varrho(M_a, M_b)_{[M_{ab}^{min}, M_{ab}^{max}]} = \int_{M_{ab}^{min}}^{M_{ab}^{max}} \varrho(M_{ab}, M_a, M_b) dM_{ab} . \quad (21)$$

The integrated two-dimensional density, (21), is a generalization of the differential density introduced in [1] for the four-pion final state. For a given invariant mass M_{ab} of the four-pion system the pair of variables (M_a, M_b) can be replaced by (Q, P_{ab}), where the Q of (10) is twice the relative three-momentum between the pions 1 and 2 in their centre-of-mass system and the relative momentum P_{ab} is equal to the total momentum of the pions 1 and 2, $P_{ab} = |\mathbf{p}_1 + \mathbf{p}_2|$, in the four-pion CMS.

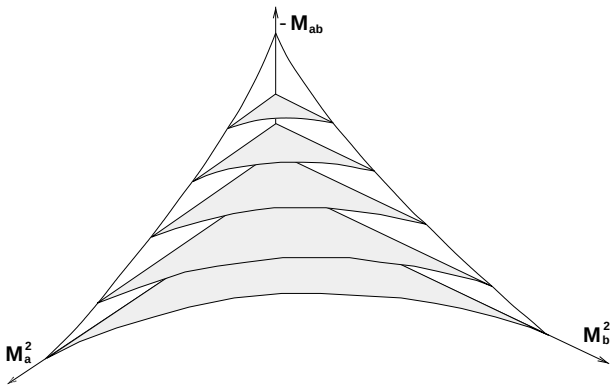

Fig. 8. The physical region in the (M_a^2, M_b^2, M_{ab}^2) space

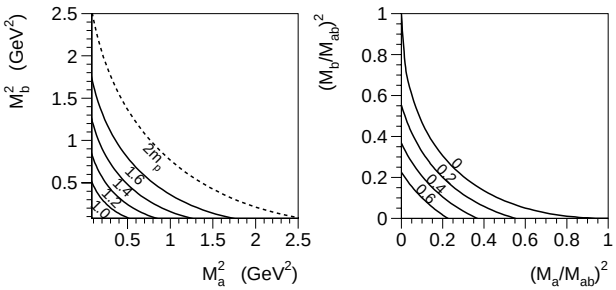

Fig. 9. **a** The physical region in the (M_a^2, M_b^2) plane for different values of the invariant mass M_{ab} (GeV) of four pions as indicated on the curves, **b** the contour plot of the relative momentum P_{ab} in the (M_a^2, M_b^2) plane. The numbers at the curves indicate the values of P_{ab}^2, (18), in units of $M_{ab}^2/4$

The physical region in the (M_a^2, M_b^2) plane depends on the invariant mass M_{ab} of the four pions, see Fig. 8. Figure 9a shows the contour plot for various values of the invariant mass M_{ab}. The region of small Q^2 where symmetrization effects are expected is in the lower left corner. The contour plot in Fig. 9b displays the relative momentum P_{ab}^2 of the two pion pairs for a given total invariant mass M_{ab}. In the relativistic phase-space approximation, the two-dimensional density $\varrho(M_a, M_b)_{[M_{ab}^{min}, M_{ab}^{max}]}$ is a superposition of flat distributions with the boundaries dependent on M_{ab} (see Fig. 9a) and $\varrho(M_a, M_b)_{[M_{ab}^{min}, M_{ab}^{max}]}$ must be flat within the physical region determined by the lower limit in the integral over M_{ab} in the r.h.s. of (21). The double-differential cross-section for the like-pion and unlike-pion pairs, $d\sigma/dM_{++}^2 dM_{--}^2$ and $d\sigma/dM_{+-(a)}^2 dM_{+-(b)}^2$, are shown in Fig. 10 in comparison with the pure phase space distribution.

In this and all similar two-dimensional plots the contrast is readjusted for clarity of graphical presentation. Wherever appropriate we shall indicate the number of events which form the basis for the subplot in question.

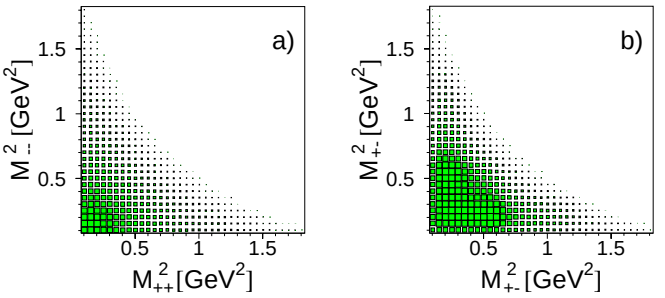

Fig. 10. The double-differential cross section *vs.* the invariant masses squared: **a** the like-pion pairs – $d\sigma/dM^2_{++}dM^2_{--}$, **b** the unlike-pion pairs – $d\sigma/dM^2_{+-}dM^2_{+-}$, **c** the pure phase space – $d\sigma/dM^2_a dM^2_b$

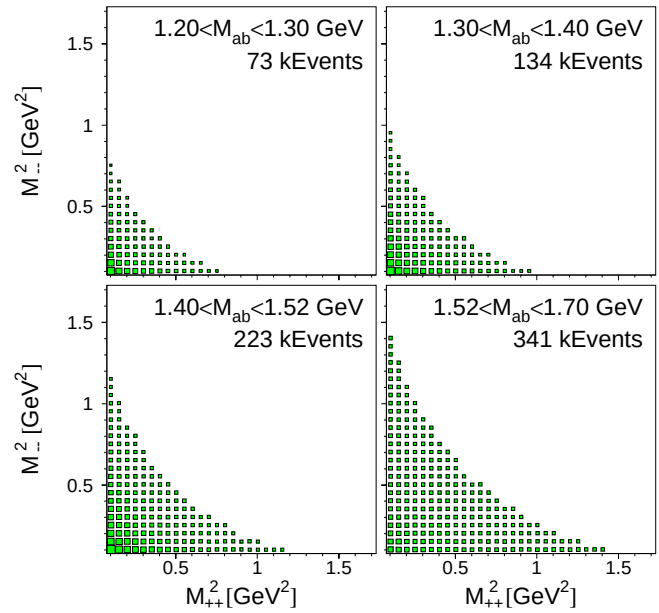

Fig. 11. The differential density $\varrho(M_{++}, M_{--})_{[M^{min}_{++--}, M^{max}_{++--}]}$ as a function of the effective masses squared of the like-pion pairs in the $2\pi^+2\pi^-\pi^0$ channel for various ranges of the $2\pi^+2\pi^-$ invariant mass as indicated. The numbers inserted in each subfigure indicate the number of events used for the calculation of ϱ

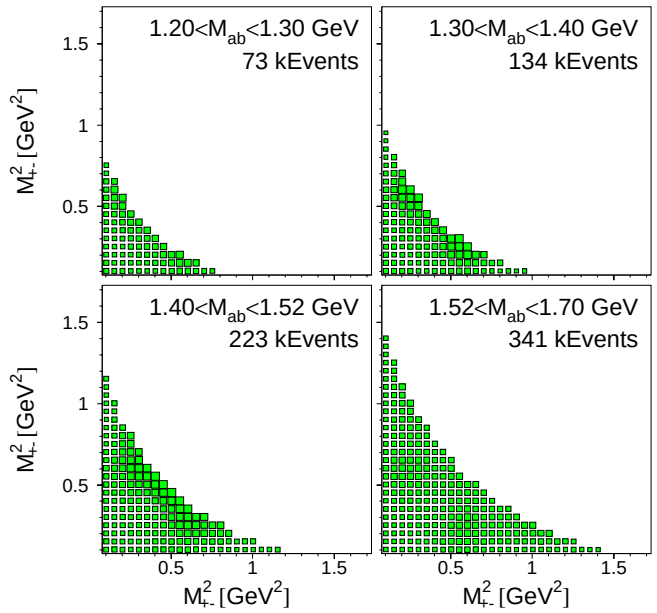

Fig. 12. The differential density $\varrho(M_{+-(a)}, M_{+-(b)})_{[M^{min}_{++--}, M^{max}_{++--}]}$ as a function of the effective masses squared of the unlike-pion pairs in the $2\pi^+2\pi^-\pi^0$ channel for various ranges of the $2\pi^+2\pi^-$ invariant mass as indicated. The numbers inserted in each subfigure indicate the number of events used for the calculation of ϱ

The number of entries in the plot is the number of events in the case of like-pion pairs and twice the number of events in the case of unlike-pairs. Recall that the total number of $2\pi^+2\pi^-\pi^0$ events is $8.3 \cdot 10^5$. In this way the reader can judge the relative importance of the data base for the graph in question.

In order to remove the trivial kinematical effects, as discussed above, we plotted the integrated differential density in Fig. 11 for *different intervals* of the $2\pi^+2\pi^-$ invariant mass $[M^{min}_{++--}, M^{max}_{++--}]$. The widths of the four chosen mass intervals $[M^{min}_{++--}, M^{max}_{++--}]$ correspond to equal volumes of the corresponding phase spaces. The dependence of these two-dimensional slices on the invariant mass of the $2\pi^+2\pi^-$ system shows an interesting effect. For the $2\pi^+2\pi^-$ mass intervals up to about 1.6 GeV, there is a clear enhancement in the double-differential density in the region of small invariant masses of the like-charge pion pairs ($M^2_{++}, M^2_{--} \to 4\mu^2$). However, no enhancement is seen for the mass interval [1.6, 1.7] GeV. This is contrary to the expectation based on a naive interpretation of the BE correlations where the strength of the peak should increase with increasing of the $2\pi^+2\pi^-$ invariant mass since the pion pairs with larger *total* momentum are better suited for probing a short range annihilation source associated with the BE effect. We shall discuss this new effect further in Sect. 4.1. The differential density $\varrho(M_{+-}, M_{+-})_{[M^{min}_{++--}, M^{max}_{++--}]}$ for the *unlike-pion pairs* is shown in Fig. 12. It displays ρ meson bands and a rather smooth behaviour below the ρ mass, as expected.

For the further discussion we construct the following partial projections (double slices) of the two-particle density. The two-dimensional space (M^2_{++}, M^2_{--}) is divided into slices $M^2_i \le M^2_{--|++} < M^2_{i+1}$ and the projections of $\varrho(M_{++}, M_{--})_{[M^{min}_{++--}, M^{max}_{++--}]}$ are defined by

$$\varrho_i(M_{++|--}) = \int_{M^2_i}^{M^2_{i+1}} \frac{\varrho(M_{++}, M_{--})_{[M^{min}_{++--}, M^{max}_{++--}]}}{\varrho^{PS}} dM^2_{--|++} \cdot \quad (22)$$

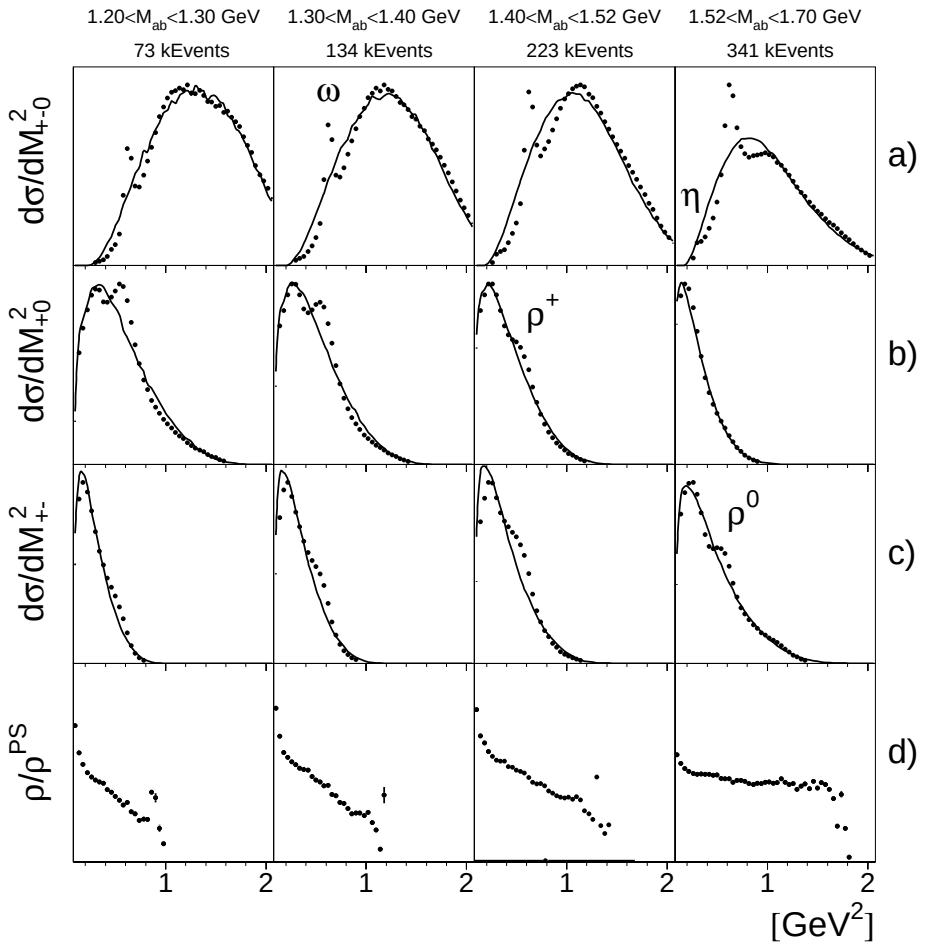

Fig. 13. The experimental mass distributions for different subsystems: **a** $\pi^+\pi^-\pi^0$ $(d\sigma/dM^2_{+-0})$, **b** $\pi^\pm\pi^0$ $(d\sigma/dM^2_{\pm 0})$, **c** $\pi^+\pi^-$ $(d\sigma/dM^2_{+-})$ together with the corresponding phase-space distributions (*solid curves*). The four columns correspond to intervals of the $2\pi^+2\pi^-$ invariant mass M_{++--} shown at the top. The numbers given above each column indicate the number of events used in that mass interval, **d** two-particle distributions (similar to $\rho_2(M)$, (8)) for the pairs of identical pions divided by the corresponding phase-space distribution

The differential density $\varrho^{PS}(M_a, M_b)$ is calculated using the five-pion phase-space samples with the experimental cuts. The pure five-pion phase-space distribution without these cuts would be a constant within the area defined by M^{min}_{++--}.

4 Discussion

4.1 Resonance effects

It is well known that resonances are strongly produced in the reaction $\bar{p}p \to 2\pi^+2\pi^-\pi^0$, see Figs. 2a–c where the signals of ρ and ω are clearly seen in the invariant mass projections. Since resonance mechanisms affect the double-differential densities (21) which we use to search for the BE correlations, it is important to investigate the role of resonance production. The strong interplay between the production of resonances and the manifestation of BE correlations is demonstrated in Fig. 13 where the inclusive mass distributions of like-pion pairs normalized to phase space are plotted for different intervals of the invariant mass M_{++--} of the $2\pi^+2\pi^-$ system. The densities have a strong peak at $M^2_{++} \to 4m^2_\pi$ for low values of M_{++--} while for the highest M_{++--} interval the distribution becomes nearly flat. This effect is strongly correlated with the relative strength of ω production as shown in Fig. 13.

To discuss the role of the $\rho\omega$ channel we introduce a kinematical cut removing the events which satisfy

$$\frac{(M_{+-} - M_\rho)^2}{(0.187\text{GeV})^2} + \frac{(M_{+-0} - M_\omega)^2}{(0.078\text{GeV})^2} \leq 1 \qquad (23)$$

for any combination of the four charged pions in the $\pi^+\pi^-$ and $\pi^+\pi^-\pi^0$ subsystems. The double-differential densities $\varrho(M_{++}, M_{--})_{[M^{min}_{++--}, M^{max}_{++--}]}$, similar to those plotted in Fig. 11, have been calculated for the data sample with the $\rho\omega$ channel removed in Fig. 14 and for the complement in Fig. 15. The double-differential densities for the events which do not contain the $\rho\omega$ channel show a clear enhancement at small invariant masses of the like-sign pion pairs for all intervals of the $2\pi^+2\pi^-$ invariant mass, while the analogous distributions for all events in Fig. 11 exhibit this feature only for a limited range of M_{++--}. Generally the distributions for the $\rho\omega$ sample of Fig. 15 are much flatter[4]. These results demonstrate that the presence or absence of BE correlations depends on the resonance channel considered. The size of BE correlations expected from certain resonance production channels is discussed in the next section.

[4] Note that the data sample in Fig. 15 contains combinatorial background events which are not of $\rho\omega$ origin

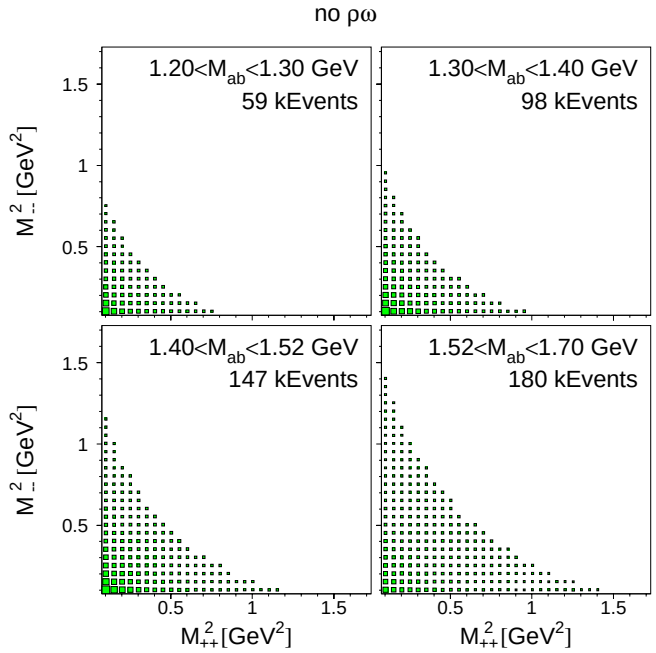

Fig. 14. The differential density $\varrho(M_{++}, M_{--})_{[M^{min}_{++--}, M^{max}_{++--}]}$ as a function of the effective masses squared of the like-pion pairs in the $2\pi^+2\pi^-\pi^0$ channel with the $\rho\omega$ events *excluded* for various ranges of the $2\pi^+2\pi^-$ invariant mass as indicated. The numbers inserted in each subfigure indicate the number of events used for the calculation of ϱ

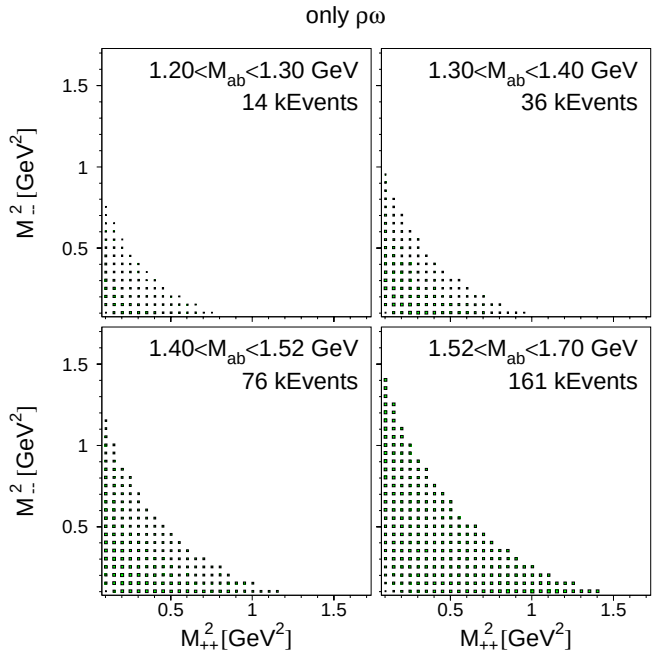

Fig. 15. The differential density $\varrho(M_{++}, M_{--})_{[M^{min}_{++--}, M^{max}_{++--}]}$ as a function of the effective masses squared of the like-pion pairs retaining only the $\rho\omega$ events in the $2\pi^+2\pi^-\pi^0$ channel for various ranges of the $2\pi^+2\pi^-$ invariant mass as indicated. The numbers inserted in each subfigure indicate the number of events used for the calculation of ϱ

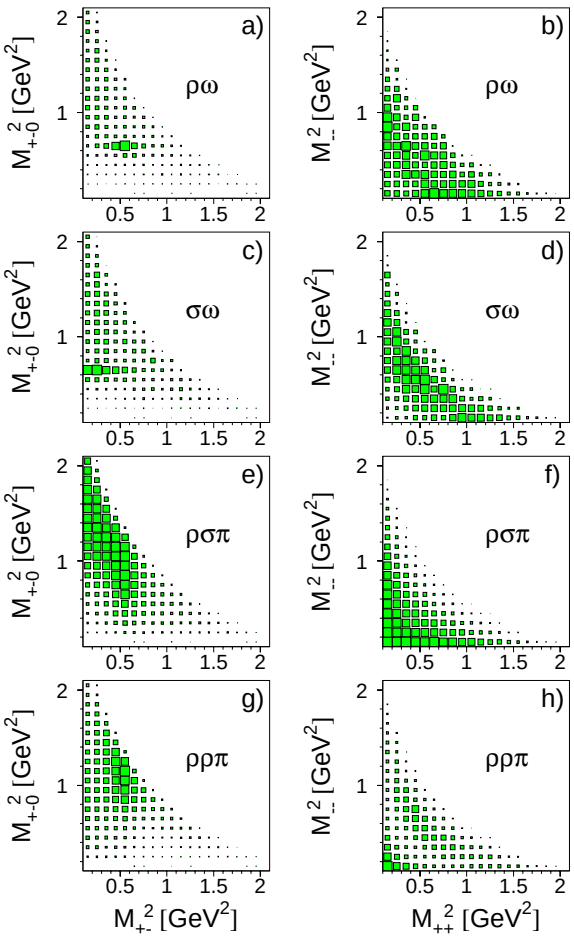

Fig. 16. The calculated mass distributions $dN/dM^2_{+-}dM^2_{+-0}$ (*left*) and the differential densities $\varrho(M_{++}, M_{--})_{[M^{min}_{++--}, M^{max}_{++--}]}$ ($M^{min}_{++--} = 1.4$ GeV) (right) for the following resonance channels: **a**,**b** $\rho^0\omega$, **c**,**d** $\sigma\omega$, **e**,**f** $\rho^0\sigma\pi^0$, **g**,**h** $\rho^0\rho^0\pi^0$. No absolute normalization is implied as the contrast is readjusted to the maximum value occurring in each plot

4.2 Model studies of the resonance effects

In this section we discuss in some detail whether the enhancement observed in $\varrho(M_{++}, M_{--})$ at $M^2_{++}, M^2_{--} \to 4\mu^2$ can be produced by resonance mechanisms. Given the large number of the essential partial waves ($^1S_0$, $^3S_1$, $^1P_1$, ^3P_J) and the complexity of the five-pion final state, a partial wave analysis would be a formidable problem which we do not attempt to solve here. Our goal is to demonstrate some typical effects arising from simple resonance mechanisms with the lowest resonances in the 2π and 3π systems. For this purpose we have performed Monte Carlo simulations of the following resonance channels: $\bar{p}p(0^{++}, 2^{++}) \to \rho^0\omega$, $\bar{p}p(1^+) \to \rho^0\pi^+\pi^-\pi^0$, $\bar{p}p(1^-) \to \sigma\omega$, $\bar{p}p(1^+) \to \rho^0\pi^0\sigma$, $\rho^\pm\pi^\mp\sigma$, $\bar{p}p(0^-) \to \rho^0\rho^0\pi^0$, $\rho^\pm\rho^\mp\pi^0$. The model amplitudes used in these calculations are described in Appendix A. The calculated mass distributions *vs.* the invariant masses of the $\pi^+\pi^-$ and $\pi^+\pi^-\pi^0$ systems and the double-differential densities for the like-pion pairs are shown in Fig. 16.

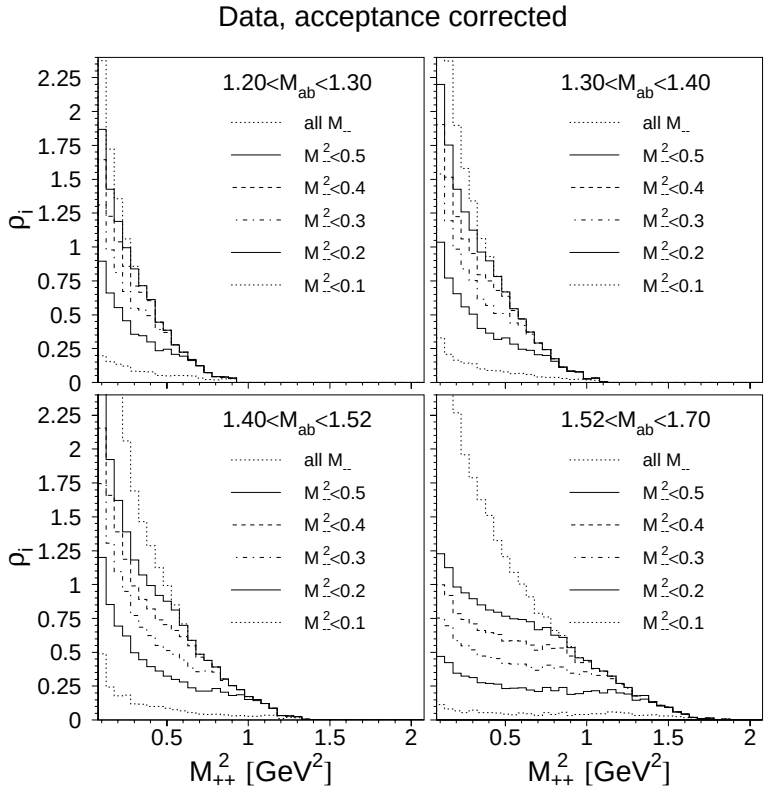

Fig. 17. The experimental projections $\varrho_i(M_{++})$ of $\varrho(M_{++}, M_{--})_{[M^{min}_{++--}, M^{max}_{++--}]}$ for the $2\pi^+2\pi^-\pi^0$ channel corrected for the detector acceptance. The $2\pi^+2\pi^-$ mass ranges are indicated in each subfigure. Different lines correspond to $(M^{max}_{--})^2$ as indicated

The mechanisms analyzed produce quite different distributions in the invariant masses of the $\pi^+\pi^-$ and $\pi^+\pi^-\pi^0$ systems as displayed in the left column of Fig. 16. Comparison with the experiment shows that the $\rho\pi\sigma$ mechanism leads to mass distributions in qualitative agreement with the data excluding the ω events. The latter can be attributed to the $\omega\rho$ and $\omega\sigma$ mechanisms.

The simulations for the differential density $\varrho(M_{++}, M_{--})$ demonstrate a strong dependence on the reaction mechanism in the region of small invariant masses M_{++} and M_{--} (the right column of Fig. 16). The $\rho\omega$ and $\sigma\omega$ mechanisms show a clear depletion of $\varrho(M_{++}, M_{--})$ for $M^2_{++}, M^2_{--} \to 4\mu^2$, therefore, these mechanisms produce no visible BE correlation effects. This result agrees with the experimental observation discussed in Sect. 4.1 that the events with ω mesons show little enhancement at small invariant masses of the $\pi^+\pi^+$ and $\pi^-\pi^-$ pairs. On the other hand, $\varrho(M_{++}, M_{--})$ at $M^2_{++}, M^2_{--} \to 4\mu^2$ shows a clear enhancement for the $\rho 3\pi$, $\rho\pi\sigma$, and $\rho\rho\pi$ mechanisms. Since overall the $\rho\pi\sigma$ mechanism (plus some ω production) is in qualitative agreement with the measured mass distributions, we conclude that at least part of the observed pion correlation signals is likely to come from resonance dynamics.

Further insight can be obtained from studying the projections $\varrho_i(M_{++})$, (22), of the differential density $\rho(M_{++}, M_{--}, M_{++--})$ as a function of the invariant masses M_{++}, M_{--}, and M_{++--}. The experimental data are shown in Fig. 17 and the simulations for the $\rho\pi\sigma$ and $\rho\rho\pi$ mechanisms in Figs. 18,19. The M_{++--} mass intervals are chosen such that the corresponding projections have the same height for the pure five-pion phase space approximation.

The amplitudes used in our model calculations have been Bose symmetrized. For the purpose of illustrating the role of quantum mechanical symmetrization we have calculated the *unphysical* case when the like-sign pions are treated as distinguishable particles. We find that for the $\rho\sigma\pi$ mechanism symmetrization plays an important role in producing the strong enhancement at small invariant mass of the like-pion pairs. This is demonstrated in Fig. 20 where the projections of the double differential densities are displayed for the *unsymmetrized* amplitude; they show no enhancement for the intermediate and high M_{++--} intervals and only moderate enhancement for the low M_{++--} interval, contrary to the symmetrized case in Fig. 18.

The importance of the resonance mechanisms for the interpretation of BE correlation signals in $\bar{p}p$ annihilation at rest has already been discussed in literature, see [12–14] and references therein. In particular, it was demonstrated [12] that the $\rho\rho - \sigma\sigma$ interference together with the BE amplitude symmetrization can satisfactorily reproduce the BE correlation peak in the $\bar{p}n \to 2\pi^+3\pi^-$ at rest. We have performed a Monte Carlo simulation of the $\rho\rho - \sigma\sigma$ interference in the state $J^{PC} = 0^{-+}$ and found that one can easily obtain double differential densities similar to the experimental ones by adjusting the relative strength and phase of the two mechanisms; a typical example is shown in Fig. 21.

Our study of the resonance mechanisms shows that the BE correlation peaks at small invariant masses of like-sign pion pairs can easily be produced either by a single channel with resonances ($\rho\sigma\pi$) or by an interference between different resonance channels ($\rho\rho\pi - \sigma\sigma\pi$), the BE sym-

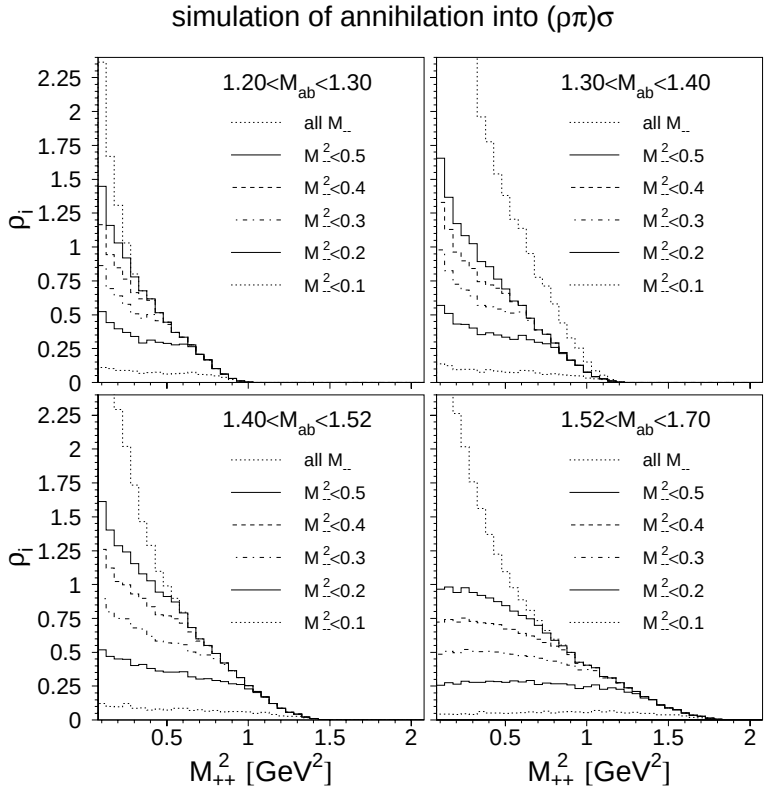

Fig. 18. The calculated projections $\varrho_i(M_{++})$ of $\varrho(M_{++}, M_{--})_{[M^{min}_{++--}, M^{max}_{++--}]}$ for the $\rho\sigma\pi$ annihilation mechanism

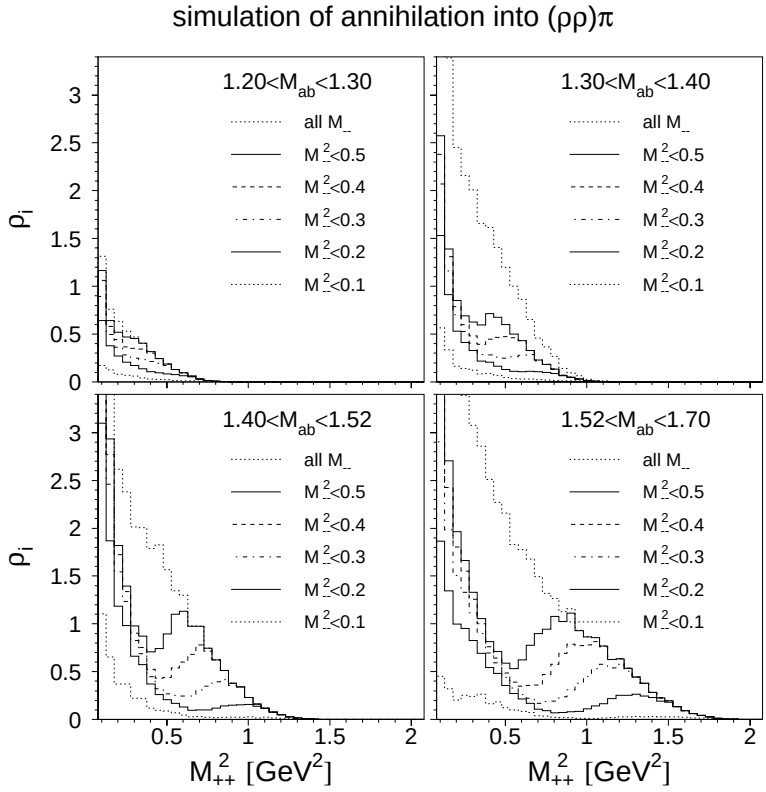

Fig. 19. The calculated projections $\varrho_i(M_{++})$ of $\varrho(M_{++}, M_{--})_{[M^{min}_{++--}, M^{max}_{++--}]}$ for the $\rho\rho\pi$ annihilation mechanism

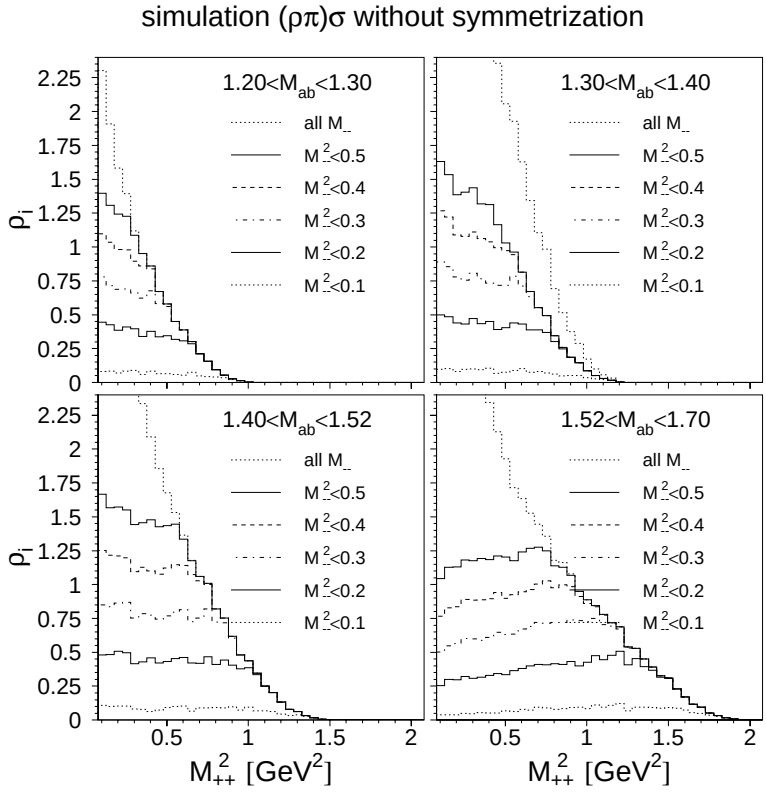

Fig. 20. The calculated projections $\varrho_i(M_{++})$ of $\varrho(M_{++}, M_{--})_{[M^{min}_{++--}, M^{max}_{++--}]}$ for the $\rho\sigma\pi$ annihilation mechanism *without Bose symmetrization*

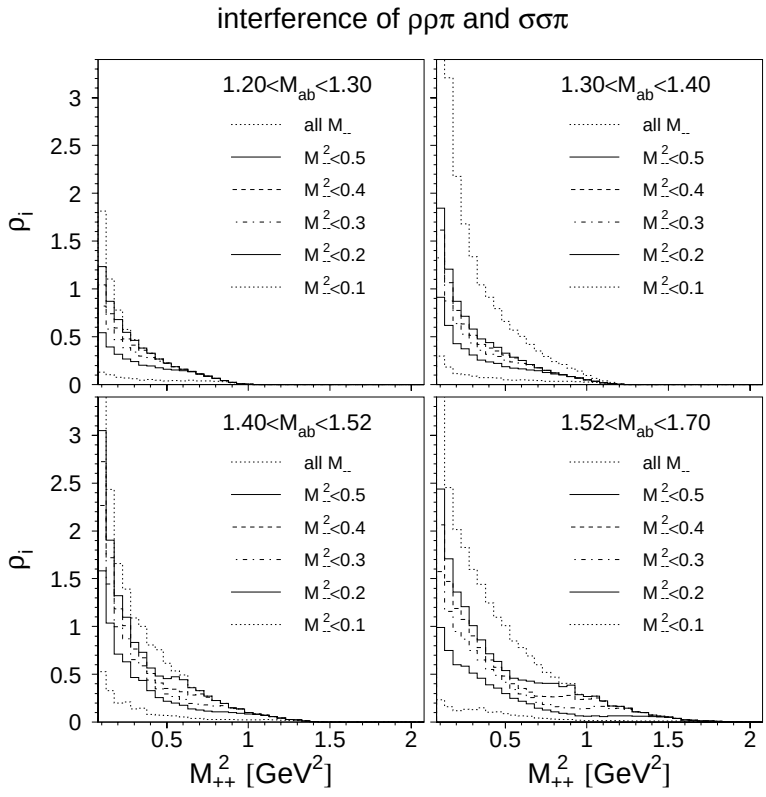

Fig. 21. The calculated projections $\varrho_i(M_{++})$ of $\varrho(M_{++}, M_{--})_{[M^{min}_{++--}, M^{max}_{++--}]}$ for the interference of the $\rho\rho\pi$ and $\sigma\sigma\pi$ annihilation mechanisms. The relative strength of the two mechanisms is normalized to equal branching ratios for the $\rho\rho\pi$ and $\sigma\sigma\pi$ channels in the absence of interference. The relative phase corresponds to maximal constructive interference at $M_{++}, M_{--} \to 2m_\pi$

metrization playing an important role in both cases. Further studies in this direction, in particular, the determination of dominant mechanisms for the individual partial waves would be very desirable.

5 Summary and conclusions

The complete kinematical information available from the CPLEAR experiment for the five pion final state in $\bar{p}p \to 2\pi^+2\pi^-\pi^0$ at rest has allowed us to study pion correlation signals for inclusive and differential distributions. The properly normalized inclusive distribution $C(M)$ for an equal charged pion pair shows a moderate enhancement at small pion pair mass. In contrast to this, the ratio $R_2(M)$ which is normalized to unequal charge pairs has a strong enhancement which however is due to the known dynamical depletion of $\pi^+\pi^-$ pairs by the nearby ρ meson resonance. Correspondingly, the direct interpretation of single variable correlation functions in terms of a pion source radius and in particular in terms of the stochastic HBT mechanism remains questionable for $\bar{p}p$ annihilation at rest as was suggested already in [1] and in earlier papers. At high energies this situation may be different [17–25].

In the 5π channel, the energy carried away by the π^0 allows us to investigate the differential distributions in the two equal charge pion pairs as a function of the $2\pi^+2\pi^-$ invariant mass. Two regimes are characteristic for the results: (1) At small π^0 energies the Dalitz plot shows a strong population by the $\rho\omega$ channel and only a weak correlation signal for small M_{++},M_{--} which is not unexpected for a two body final state. (2) The larger part of the data corresponding to sizable π^0 energies is characterized by the dominance of the $\rho 3\pi$ channel in the Dalitz plot. It shows a large correlation enhancement at low M_{++},M_{--} similar to the situation occurring in the $\bar{p}p \to 2\pi^+2\pi^-$ channel analyzed in the earlier paper [1]. Theoretical simulations of the $\rho 3\pi$ and $\rho\sigma\pi$ channel show an enhancement in the M_{++},M_{--} correlation corner which is qualitatively similar to the observed effect. By studying partial projections of the differential correlation signals, this enhancement has been traced to the P-wave nature of the ρ meson resonance in combination with the trivial quantum mechanical Bose symmetrization of the resonance production amplitude. A fair amount of the observed correlation enhancement may therefore be due to conventional resonance production amplitudes which are however difficult to normalize absolutely. We therefore have refrained from making any fits related to pion source radii both for the inclusive distributions where the signal is relatively weak and also for the double-differential correlation functions where a good part of the enhancement is likely to be due to resonance production mechanisms. The simulations made in the earlier analysis [1] for the $2\pi^+2\pi^-$ channel produced no major contribution to the correlation signals coming from the $\rho\pi\pi$ and $\rho\rho$ mechanisms. In view of the present situation a simultaneous full partial wave analysis of the $2\pi^+2\pi^-$, of the $2\pi^+2\pi^-\pi^0$ and of the multiple π^0 channels would be desirable. This is however beyond the scope of this paper.

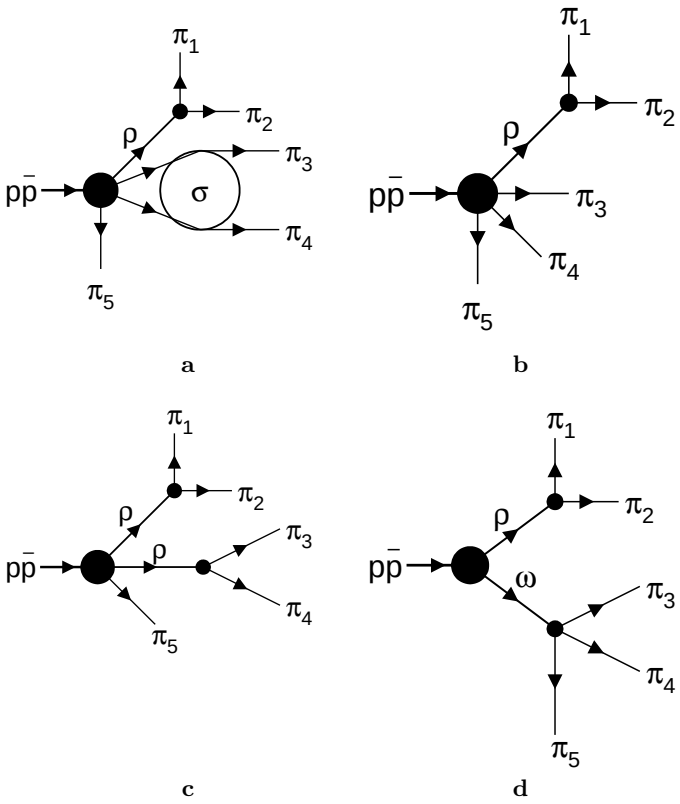

Fig. 22a–d. Resonance mechanisms of the $\bar{p}p$ annihilation into 5π

Acknowledgements. We would like to thank the CERN LEAR staff as well as the technical and engineering staff of our institutes for their support and co-operation. This work was supported by the following institutions: the French CNRS/Institut National de Physique Nucléaire et de Physique des Particules, the French Commissariat à l'Energie Atomique, the Greek General Secretariat of Research and Technology, the Netherlands Foundation for Fundamental Research on Matter (FOM), the Portuguese JNICT, the Ministry of Science and Technology of the Republic of Slovenia, the Swedish Natural Science Research Council, the Swiss National Science Foundation, the UK Particle Physics and Astronomy Research Council (PPARC), and the US National Science Foundation.

A Appendix

The amplitudes corresponding to the resonance mechanisms $\rho\pi\sigma$, $\rho 3\pi$, $\rho\rho\pi$,and $\rho\omega$ are given by the diagrams in Fig. 22.

The $\bar{p}p$ vertices are taken with a minimum number of derivatives. The $\rho\pi\pi$ vertex has the form

$$V_{\rho\pi\pi} = g_1 \epsilon_\mu (p_1^\mu - p_2^\mu) F_{\rho\pi\pi}(m_{\pi\pi}^2) \qquad (24)$$

where g_1 is the coupling constant, ϵ_μ is the polarization of the ρ, p_n^μ are the pion momenta, and $F_{\rho\pi\pi}(m_{\pi\pi}^2)$ is the form factor depending on the invariant mass of the $\pi\pi$ system. In similar notation, the $\omega\pi\pi\pi$ vertex has the form

$$V_{\omega\pi\pi\pi} = g_2 \varepsilon_{\mu\alpha\beta\gamma} \epsilon^\mu p_1^\alpha p_2^\beta p_3^\gamma \quad . \qquad (25)$$

The propagators corresponding to the vector particles are given by the formula

$$G(p) = \frac{g^{\mu\nu} - p^\mu p^\nu / m_V^2}{p^2 - m_0^2 - \mathcal{M}(p^2)} \tag{26}$$

where m_V and m_0 are the physical and bare masses and $\mathcal{M}(p^2)$ is the mass operator. The mass operator for the ρ meson is defined by the dispersion integral:

$$\mathcal{M}(s) = \frac{1}{2\pi} \int_{4m_\pi^2}^{\infty} \frac{\Gamma(s')}{s - s'} ds' \tag{27}$$

$$\Gamma(s) = \frac{g_1^2 F_{\rho\pi\pi}(s)^2 k^3}{24\pi s} \tag{28}$$

where $k = \sqrt{s/4 - m_\pi^2}$ is the relative momentum in the $\pi\pi$ system. A monopole form factor $F_{\rho\pi\pi}(s) = (1 + k^2/\nu^2)^{-1}$ is used with $\nu = 0.2$ GeV, and the parameters m_0 and g_1 are defined by the mass and the width of the ρ meson. The energy dependence of the mass operator for the ω meson is neglected: $m_0^2 + \mathcal{M}(p^2) = (m_\omega - i\Gamma_\omega/2)^2$ with constant Γ_ω.

The σ block in Fig. 22a denotes the full Green function of the $\pi\pi$ system in the scalar-isoscalar channel. The coupled channel model [16] has been used to describe the S-wave $\pi\pi$ final state interaction which leads to an additional factor proportional to the pion scalar form factor $F_\pi^0(s_{\pi\pi})$ (see [16] for details).

The components above are combined straightforwardly to construct the amplitudes for the resonance channels concerned. For example, the amplitude corresponding to the $N\bar{N}(J^{PC} = 1^{+-}, I = 0) \to \rho\sigma\pi$ has the following structure:

$$T_{N\bar{N}\to\rho\sigma\pi\to5\pi} = g_a g_1 \frac{F_\pi^0(m_{34}^2)}{m_{12}^2 - m_0^2 - \mathcal{M}(m_{12}^2)} \times \epsilon_\mu^a (p_1^\mu - p_2^\mu) C^{1\nu_5}_{1\nu_1 1\nu_2} C^{00}_{1\nu_3 1\nu_4} \quad . \tag{29}$$

Here $m_{nk} = (p_n + p_k)^2$ and ν_n are the isospin indices of the pions. To obtain the proper amplitude the expression on the r.h.s of (29) must be symmetrized with respect to all permutations of the pions. The amplitudes for the other resonance mechanisms: $N\bar{N}(J^{PC} = 1^{+-}, I = 0) \to \rho 3\pi$, $N\bar{N}(J^{PC} = 0^{-+}, I = 1) \to \rho\rho\pi$, $N\bar{N}(J^{PC} = 0^{-+}, I = 1) \to \sigma\sigma\pi$, $N\bar{N}(J^{PC} = 0^{++}, I = 1) \to \rho\omega$ are constructed in a similar way

$$T_{N\bar{N}\to\rho\pi\pi\pi\to5\pi} = g_a g_1 \frac{1}{m_{12}^2 - m_0^2 - \mathcal{M}(m_{12}^2)} \times \epsilon_\mu^a (p_1^\mu - p_2^\mu) C^{1\nu_5}_{1\nu_1 1\nu_2} C^{00}_{1\nu_3 1\nu_4} \tag{30}$$

$$T_{N\bar{N}\to\rho\rho\pi\to5\pi} = g_a g_1^2 \frac{(p_1 - p_2)^\mu (p_3 - p_4)_\mu}{(m_{12}^2 - m_0^2 - \mathcal{M}(m_{12}^2))\,(m_{34}^2 - m_0^2 - \mathcal{M}(m_{34}^2))} \times \sum_\nu C^{1\nu}_{1\nu_1 1\nu_2} C^{1\,-\nu}_{1\nu_3 1\nu_4} \delta_{\nu_a\nu_5} \tag{31}$$

$$T_{N\bar{N}\to\sigma\sigma\pi\to5\pi} = g_a F_\pi^0(m_{12}^2) F_\pi^0(m_{34}^2) C^{00}_{1\nu_1 1\nu_2} C^{00}_{1\nu_3 1\nu_4} \delta_{\nu_a\nu_5} \tag{32}$$

$$T_{N\bar{N}\to\rho\omega\to5\pi} = g_a g_1 g_2 \frac{\epsilon_{\mu\alpha\beta\gamma}(p_1 - p_2)^\mu p_3^\alpha p_4^\beta p_5^\gamma}{(m_{12}^2 - m_0^2 - \mathcal{M}(m_{12}^2))\,(m_{34}^2 - m_\omega^2 - i m_\omega \Gamma_\omega)} \times C^{1\nu_a}_{1\nu_1 1\nu_2} C^{1\,-\nu_5}_{1\nu_3 1\nu_4} \ . \tag{33}$$

Here g_a is the coupling constant for the corresponding $N\bar{N}$ annihilation vertex, $C^{t\nu}_{t_1\nu_1 t_2\nu_2}$ are the Clebsch-Gordan coefficients, ν_a is the isospin component of the initial state with the isospin $I = 1$, and the proper BE symmetrization is implied.

References

1. A. Angelopoulos et al., CPLEAR Collaboration, Europ. Phys. J. **C1** (1998) 139
2. R. Hanbury-Brown, R.Q. Twiss, Phil. Mag. **45**, 633 (1954)
3. G. Goldhaber et al., Phys. Rev. Lett. **3**, 181 (1959); G. Goldhaber et al., Phys. Rev. **120**, 300 (1960)
4. G. Cocconi, Phys. Lett. B **49**, 459 (1974)
5. G.I. Kopylov, M.Y. Podgoretskii, Sov. J. Nucl. Phys. **19**, 215 (1974)
6. R. Adler et al., CPLEAR Collaboration, Phys. Lett. B **267**, 154 (1991); R. Adler et al., CPLEAR Collaboration, Z. Phys. C **65**, 199 (1995)
7. R. Adler et al., CPLEAR Collaboration, Nucl. Instrum. Methods A **379**, 76 (1996)
8. R. Adler et al., CPLEAR Collaboration, Z. Phys. C **63**, 541 (1994)
9. M. Deutschmann et al., Nucl. Phys. B **204**, 333 (1982)
10. S. Ahmad et al., Proc. IV LEAR Workshop, Villars (1987) 697, edited by C. Amsler, G. Backenstoss, R. Klapisch, C. Leluc, D. Simon, L. Tauscher
11. K. Sarigiannis et al., Nucl. Phys. A **558**, 43c (1993)
12. M. Gaspero, Nucl. Phys. A **588**, 861 (1995); A **614**, 565 (1997)
13. M. Gaspero, A. De Pascuale, Phys. Lett. B **358**, 146 (1995)
14. P. Annios et al., Phys. Rev. **20**, 402 (1968)
15. H.Q. Song, B.S. Zou, M.P. Locher, J. Riedlberger, P. Truöl, Z. Phys. A **342**, 439 (1992)
16. M.P. Locher, V.E. Markushin, H.Q. Zheng, Phys. Rev. D **55** (1997) 2894
17. A. Breakstone et al., Phys. Lett. B **162**, 400 (1985)
18. T. Alexopoulos et al., Phys. Rev. D **48**, 1931 (1993)
19. P. Abreu et al., DELPHI Collaboration, Z. Phys. C **63**, 17 (1994)
20. T. Akesson et al., Phys. Lett. B **129**, 269 (1983)
21. T. Akesson et al., Phys. Lett. B **187**, 420 (1987); T. Akesson et al., Z. Phys. C **36**, 517 (1987)
22. C. Albajar et al., Phys. Lett. B **226**, 410 (1989)
23. N. Neumeister et al., Phys. Lett. B **275**, 186 (1992)
24. N. Neumeister et al., Z. Phys. C **60**, 633 (1993)
25. T.C. Awes et al., Z. Phys. C **69**, 67 (1995)